GEOPHYSICAL RESEARCH LETTERS, VOL. 25, NO. 20, PAGES 3815-3818, OCTOBER 15, 1998

# A use of two-channel radiances for an aerosol characterization from space

Teruyuki Nakajima and Akiko Higurashi[1]

Center for Climate System Research, University of Tokyo, Tokyo, Japan

**Abstract.** We report new satellite retrievals of an aerosol particle size index, Ångström exponent, along with aerosol optical thickness, obtained from a two channel algorithm for NOAA/AVHRR and ADEOS/OCTS satellite-borne radiometers. The results show characteristic features of the global aerosol size index on global scale. Small aerosol particles were detected in fairly large-scale areas around mid-latitude industrial regions and tropical biomass burning regions, whereas large aerosol particles were detected over most of the ocean area and over subtropical arid areas.

## Introduction

It has been some time since scientists recognized that anthropogenic aerosols can influence the earth's climate significantly. Direct and indirect effects of aerosols are evaluated as comparably large as the radiative forcing of greenhouse gases but with negative sign [*IPCC95*, 1996]. Recent evaluation of global aerosol effects is, however, based mostly on the aerosol optical thickness distribution retrieved from red channel radiances of AVHRR [*Husar et al.*, 1997] and geostational satellites [*Moulin et al.*, 1997], apart from model estimation with fossil fuel consumption [*Langner et al.*, 1992]. In spite of valuable contributions of the satellite methods, detection of optically thin aerosol signature is difficult only with one channel of a radiometer. Especially, it is difficult to detect anthropogenic aerosol layers which are much thinner than dust layers in subtropical arid regions. The typical aerosol optical thickness off New York area is of order of 0.1 for which the radiative forcing at the top of the atmosphere will be of order of 2 W/m$^2$ [*Husar et al.*, 1997; *Stowe*, Personal communication, 1997]. To improve the above mentioned difficult situation, we discuss a use of a two channel algorithm applied to data of NOAA/AVHRR and ADEOS/OCTS radiometers.

## Aerosol characterization from space

Direct and ground-based remote sensing measurements of aerosols [*Patterson and Gillette*, 1977; *Nakajima et al*, 1989; *Kaufman et al.*, 1994] have shown there is a strong correlation between the aerosol type and the typical aerosol particle size. Soil-derived and sea-salt aerosols will have a micron order radius, whereas accumulation mode aerosols, created by gas-to-particle conversion, tend to have a sub-micron radius. The typical particle radius of accumulation mode aerosols is remarkably similar among measured values, i. e., ~0.2 μm. Since the optical thickness spectrum is almost uniquely related with the aerosol size distribution, the following Ångström's law is another expression for sizing aerosols [*Ångström*, 1961]:

$$\tau_\lambda = \beta \lambda^{-\alpha}, \tag{1}$$

where $\tau_\lambda$ is the aerosol optical thickness at wavelength $\lambda$. The constants $\beta$ and $\alpha$ are called the Ångström's turbidity factor and exponent, respectively. In this paper we rather use the aerosol optical thickness at wavelength of 0.5 μm, $\tau_{0.5}$, transformed from $\beta$ as $\tau_{0.5} = \beta\, 0.5^{-\alpha}$. The electromagnetic scattering theory indicates that small particles with radius comparable to $\lambda$ have large $\alpha$ values of order of 1, while large particles have small $\alpha$ values close to 0. The typical observed value for $\alpha$ is ~1 for small urban-type aerosols and ~0 for large soil-derived particles [*Tanré*, 1988; *Nakajima et al.*, 1989; *Kaufman et al.*, 1994]. Thus, a scatter diagram of $\alpha$ vs $\tau_{0.5}$ is useful for an optical characterization of aerosols in terms of the typical particle size and the total cross section of aerosol polydispersion.

Ångström parameters, $\alpha$ and $\tau_{0.5}$, can be obtained from space if we have two wavelengths of a satellite-borne radiometer in a manner similar to sunphotometry and sky-radiometry [*Nakajima et al.*, 1996; *Holben et al.*, 1996]. For this purpose we have developed a two channel algorithm using spectral radiances in AVHRR red-channel (channel-1, $\lambda$= 0.63μm) and near-IR channel (channel-2, $\lambda$= 0.91 μm) [*Nakajima and Higurashi*, 1996; *Higurashi and Nakajima*, 1998]. In the algorithm we have assumed a complex refractive index of aerosols as $m$ = 1.5 - 0.005$i$ and a bimodal size distribution,

$$\frac{dV}{d\ln r} = \sum_{n=1}^{2} C_n \exp\{-\frac{1}{2}[\frac{\ln r - \ln r_n}{\sigma_n}]^2\}. \tag{2}$$

We feel this type of size distribution is more realistic than the power law type size distribution, since it can simulate a saddle point feature of the tropospheric aerosol size distribution around $r$ ~ 0.6 μm. Two peak volumes of the modes, $C_1$ and $C_2$, are left as undetermined parameters to be retrieved from satellite-received radiances. Assuming the Mie theory we made look-up tables of apparent reflectances in channel-1 ad -2 of AVHRR as a function of $\tau_{0.5}$ and $\alpha$, because those parameters are uniquely related with $C_1$ and $C_2$ as discussed above. Assuming trial values $\tau_{0.5}$ and $\gamma$, theoretical reflectances in channel-1 and -2 of AVHRR are constructed by the look up tables to be compared with observed reflectances. The optimal values of $\tau_{0.5}$ and $\gamma$, that minimize the root mean square deviation $\varepsilon$ between observed and theoretical reflectances, are searched by an iteration method until $\varepsilon$ becomes less than 0.0001 for each channel.

For various corrections in the algorithm, we use SSM/I-retrieved ocean surface wind velocity, TOMS-retrieved ozone amount, and ECMWF objective analysis water vapor profile.

[1]Now at National Institute for Environmental Studies, Tsukuba, Japan.



Paper number 98GL02151.
0094-8276/98/98GL-02151$05.00

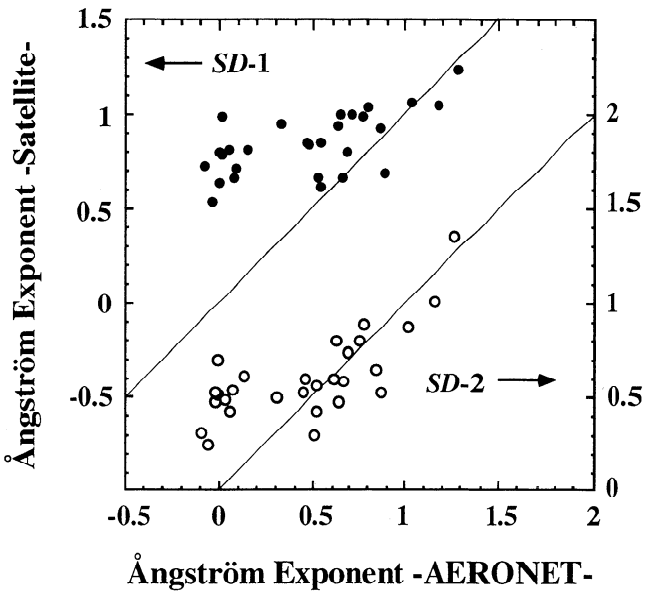


**Figure 1.** A comparison of satellite-derived Ångström exponents with values obtained from sunphotometry of AERONET. Each point corresponds to a monthly average of satellite-derived Ångström exponent values (year of 1990) and ground-based values (a period of 1995-1997). Results with two size distributions *SD*-1 and *SD*-2 are shown with an ordinate shift of $\Delta\alpha = 1$ for *SD*-2 to separate two data groups.

Data are avoided with surface wind velocity larger than 15 m/s and the cone angle less than 40° in order to get rid of the effect of whitecaps and sun-glint. According to numerical simulations, the expected retrieval error in the Ångström exponent is less than 0.2, when $\tau_{0.5} > 0.1$, for errors such as a 2 g/cm$^2$ error in the assumed water vapor amount or a 3 km error in the assumed geometrical thickness of the aerosol layer.

Extensive analyses of real satellite data have indicated that a suitable setting of parameters appeared in Eq. (2) is important for successful retrievals of Ångström parameters on global scale. *Higurashi and Nakajima* [1998] assumed $r_1$=0.17 μm, $\sigma_1$= 0.67, $r_2$= 3.44 μm, and $\sigma_2$= 0.86, as the averages of reported size distributions [e. g., *Patterson and Gillette*, 1977; *Nakajima et al.*, 1989; *Shiobara et al.*, 1991]. This size distribution is referred to as *SD*-1 hereafter. Figure 1 compares satellite-retrieved Ångström exponents assuming *SD*-1 with ground-based values obtained from AERONET, an automatic sky radiometer network operated by NASA [*Holben et al.*, 1996]. Such a comparison will be useful for validating the present algorithm, even though the year of comparison is different from each other (AERONET has been set after 1994), since the relative shape of the aerosol size distribution will be characteristic depending on each area's aerosol sources as compared to the aerosol concentration. It is found in Fig. 1 that the size distribution *SD*-1 produces a fairly good agreement between satellite-retrieved and ground-based values for relatively large $\alpha$, whereas there is a group of small ground-based values which cannot be retrieved in proper manner by the present algorithm. In order to improve the result, we adopt in this paper a tuned size distribution *SD*-2 defined by Eq. (2) with $\sigma_1$= 0.26 and $\sigma_2$= 1.01. On the other hand, the tuned size distribution *SD*-2 reduces the disagreement, although there are still overestimation by satellite. Root mean square differences between satellite-derived and AERONET-observed Ångström exponents are 0.31 and 0.48 for *SD*-1 and *SD*-2, indicating the tuned size distribution *SD*-2 is better for retrieving Ångström exponent. Since deviations become 0.15 and 0.20 if data are limitted to $\alpha > 0.5$, the present retrieval system is reliable for obtaining Ångström exponent of anthropogenic sulfate aerosols and biomass burning aerosols.

Small $\alpha$ values in Fig 1 orignate from areas of prevailing soil-derived particles such as the ocean area next to the Saharan desert. There are several possible causes of overestimation of the Ångström exponent for mineral dust layer cases. *Nakajima et al.* [1989] found a significant difference in the measured phase function of Chinese yellow dust particles by a polar nephelomete from that of Mie spherical scattering approximation, whereas *Tanré et al.* [1988] found Mie scattering theory can fit the sky radiance distribution fairly well for Saharan dust particles. Difference in water vapor uptake by mineral dust particles can cause such a difference in nonsphericity of particles. In order to make a rough estimation of the effect of nonsphericity on the present retrieval, we have made a test calculation with a non-spherical model of Chinese yellow sand particles with the semi-empirical scattering theory of *Pollack and Cuzzi* [1980]. Although such a semi-empirical theory may not be perfect for the test, the test result is suggestive that nonspherical scattering effect may not be large for retrievals of the Ångström exponent. This can be understood because the wavelength dependence of the phase function does not change much from that of Mie theory, as far as the refractive index is same at these wavelengths. Therefore, we are rather suspecting that the problem originates from our assumption of the same refractive index in two channels, although it is difficult to find a systematic wavelength dependence of the complex refractive index of mineral dust particles in the reported values at these wavelengths [e. g., *Sokolik et al.*, 1993].

## Global distributions of Ångström parameters

Figure 2 shows global distributions of the Ångström parameters with 0.5° spatial resolution over ocean obtained by NOAA/AVHRR-11 (panel-a) and ADEOS/OCTS (panel-b) with the present two channel algorithm. AVHRR-retrievals are for the annual mean values of Ångström parameters in 1990 and OCTS-retrievals are for the monthly mean values in April, 1997. The present algorithm can be applied to channel-6 and -8 ($\lambda$ = 0.667 and 0.862 μm) radiances of OCTS without difficulty, since analyses of those channel radiances are easier than those of AVHRR with band widths much narrower than those of AVHRR channel-1 and -2.

An interesting observation in Fig. 2 is that the northern middle latitudes tend to have a large Ångström exponent in the summer season. If we make a scatter plot of $\alpha$ vs $\tau_{0.5}$ as in Fig. 3, it is quite consistent with the growth pattern of accumulation mode aerosols in the urban type airmass observed by ground-based measurements [*Nakajima et al.*, 1989; *Kaufman and Holben*, 1996]. Accumulation of fresh gas-to-particle conversion aerosols will increase both the optical thickness and the Ångström exponent (i. e., a positive correlation between $\tau_{0.5}$ and $\alpha$), whereas the growth of aerosols absorbing water vapor will increase the optical thickness and decrease the Ångström exponent (i. e., a negative correlation between $\tau_{0.5}$ and $\alpha$). Typical $\alpha$ values range 0.5 ~ 1 in these processes. Consistently, high $\alpha$ values occur in Fig. 2 around industrial

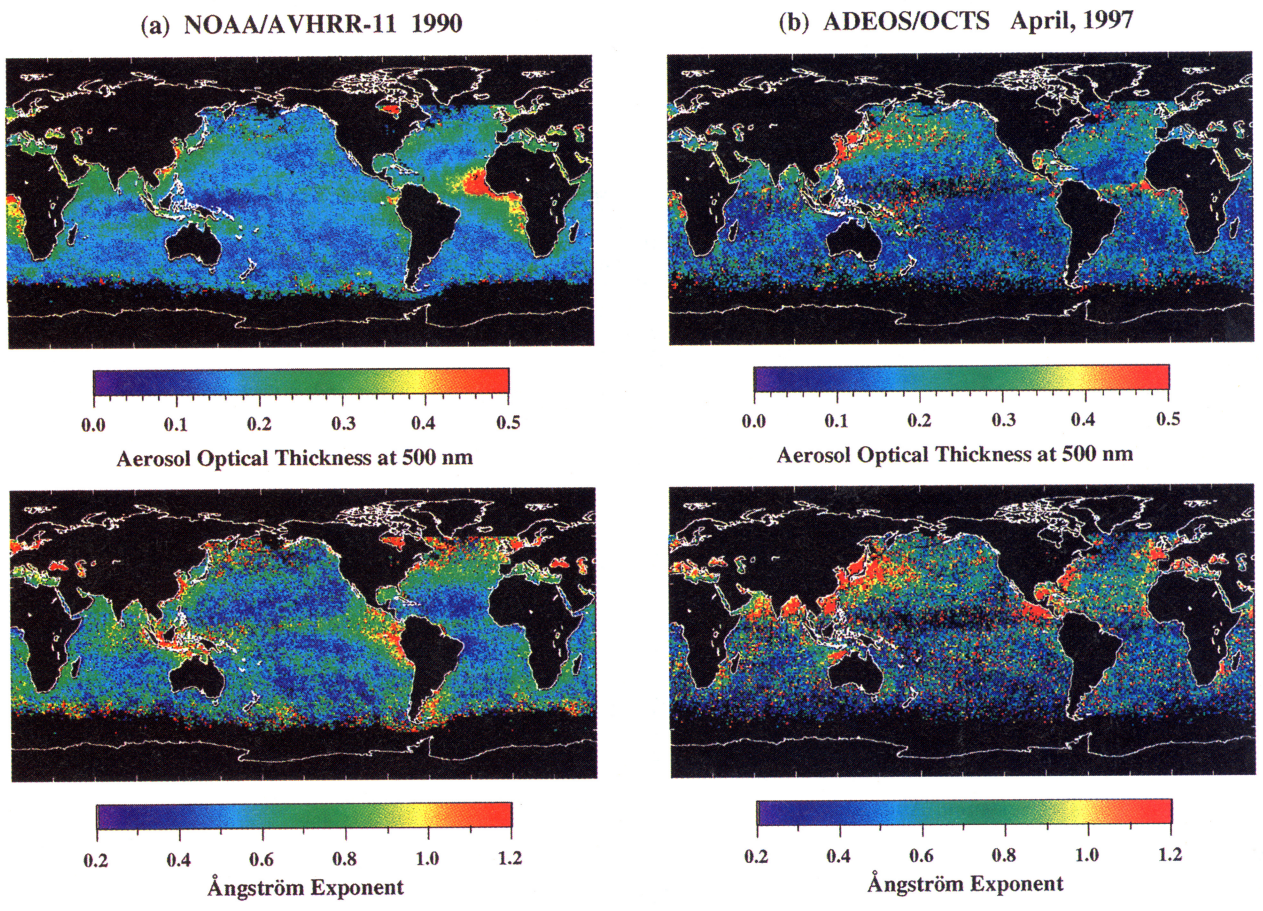


**Figure 2.** Global distributions of the aerosol optical thickness at $\lambda = 0.5$ μm and Ängström exponent derived by a two channel satellite algorithm. Results are shown for annual mean values in 1990 with AVHRR-11 channel-1 and -2 radiances (a), and one month mean values in 1997 with ADEOS/OCTS channel-6 and -8 radiances (b).

areas such as the east coast of USA, China, Mediterranean Sea, and Black sea. Thus we may conclude that we are observing anthropogenic aerosols by large Ängström exponent values in Fig. 2. If this is as it is, the transportation length of anthropogenic aerosols is quite large as several 1000 km. Note that it is very difficult to find such transportation pattern only with a monthly optical thickness distribution.

There are other areas with large Ångström exponent values off the west coasts of South Africa, Central and South America, and Indonesia-Northern Australian areas. Comparing with forest fire distributions [*Andreae*, 1993] and TOMS UV-absorbing aerosol distributions [*Herman et al.*, 1997], we conclude that those large $\alpha$ values are caused by biomass burning aerosols. A ground-based sky radiometry has shown a significant increase in submicron particle volume in the biomass burning season of Amazon region [*Holben et al.*, 1996]. Gas-to-particle conversion phenomenon of carbonaceous aerosols is one of interesting topics for future studies [*Penner and Novakov*, 1996]. It is also quite impressive in Fig. 2 to see a strong contrast of $\alpha$ along the west coast of South America, indicating the dominant particle radius changes from small to large between southern and northern areas. This contrast seems to correspond to a contrast between dominating climates in wet Selvas-Amazon area and arid Andes-Pampa area. In this regard it is also interesting to see that the South African aerosol layer tends to have a large particle size, different from South American aerosols. This might indicate that aerosols in this area are of a mixture of biomass burning small aerosols with large soil-derived particles. Another interesting feature in Fig. 2 is a slight rise of $\alpha$ in the tropical convergence zone. There is a proposal that small sulfate particles are generated in the tropical ocean area from biological activities [*Charlson et al*, 1987; *Durkee et al.*, 1991]. It should be noted, however, that Fig. 2 does not show a rise of the $\alpha$ value in the tropical area as large as shown by *Durkee et al.* [1991]. Rather, most of the ocean area have small $\alpha$ values consistent with the experience in ocean color remote sensing [*Evans and Gordon*, 1994]. The distribution pattern of $\alpha$ in Fig. 2 suggests that optically effective small particles in tropical ocean areas are mainly originated from biomass burning processes. We should investigate why we have such differences in evaluation of the small particle concentration depending on studies.

Judging by the distribution pattern of $\alpha$ value in Figs. 2 and 3, small Ängström exponent values correspond obviously to soil-derived aerosols emitted from subtropical arid areas. The scatter plot in Fig. 3 shows $\alpha$ values tend to be independent of $\tau_{0.5}$ as consistent with ground-based values.

## Conclusions and future perspectives

As discussed in the preceding sections, the present retrievals of Ängström parameters look reliable for a global charac-

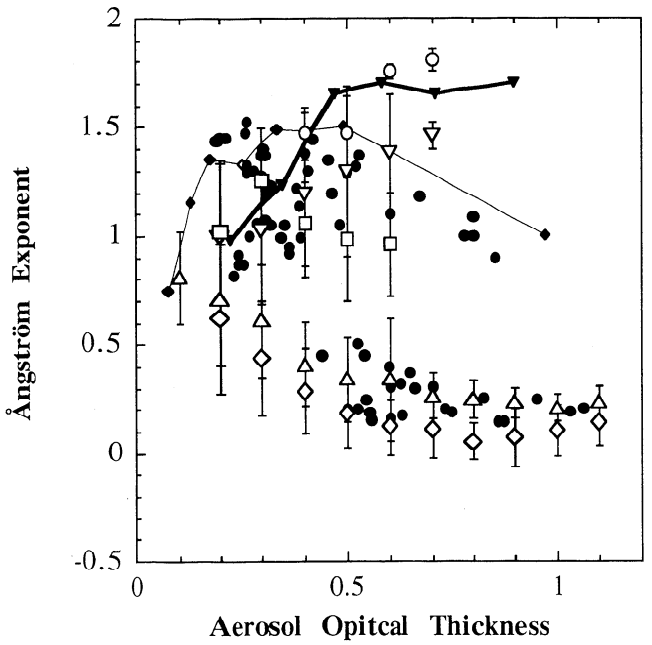


**Figure 3.** Scatter plots of Ångström exponent $\alpha$ vs turbidity factor $\tau_{0.5}$. Ground-based values are obtained by sunphotometry and sky radiometry (*Nakajima et al.*, 1989; *Kaufman and Holben*, 1996). This study: ○ Black Sea, July: ◇ Arabian Sea, July; ▽East coast of North America, April; △West coast of North Africa, Oct.; □East coast of South China, April. Ground-based sunphotometry: ● *Nakajima et al.* (1989); —◆—*Kaufman and Holben* (1996), Eastern US; —▼—*Kaufman and Holben* (1996), Deforestation, Aug.-Sept.

terization of aerosols. Even though the algorithm has some difficulty in retrieving proper Ångström exponents of soil-derived aerosols, a combination of the optical thickness and Ångström exponent is significantly effective to identify small and large aerosol distributions. Distribution patterns of small and large particles depict large scale transportation of small mid-latitude anthropogenic aerosols and subtropical biomass burning aerosols, as well as well known transportation of large mineral dust aerosols.

A global size index is also of great help for calculating the aerosol number density, which is necessary for evaluation of the Towmey mechanism [*Twomey*, 1977] and Albrecht mechanism [*Albrecht*, 1989] in studies of cloud-aerosol interaction phenomena. In very near future, there will be a great progress of aerosol and cloud remote sensing with recent and planned satellite missions.

**Acknowledgments.** The authors are grateful to L.L. Stowe of NOAA NESDIS for comments on retrieval algorithms; B.N. Holben and A. Smirnov of NASA GSFC for providing AERONET data for validation; C.J. Tucker of NASA GSFC and New Energy and Industrial Technology Development Organization of Japan for providing AVHRR GAC data. This research was supported by Grant-in-Aid for Scientific Research on Priority Areas (No. 08241104) of Japanese Ministry of Education, Science, Sports and Culture; by NASDA ADEOS/OCTS project.

## References

Albrecht, B.A., Aerosols, cloud microphysics, and fractional cloudiness, *Science, 245*, 1227-1230, 1989.

Ångström, A., Techniques of determining the turbidity of the atmosphere, *Tellus, 13*, 214-223, 1961.

Andreae, M.O., Global distribution of fires seen from space, *Eos. Trans. Ameri. Geophys., 74*, 129-144, 1993.

Charlson, R.J., J.E. Lovelock, M.O. Andreae, and S.G. Warren, Oceanic phytoplankton, atmospheric sulphur, cloud albedo and climate, *Nature, 326*, 655-661, 1987.

Durkee, P.A., F. Pfeil, E. Frost, R. Shema, Global Analysis of Aerosol Particle Characteristics, *Atmos. Environ., 25A*, 2457-2471, 1991.

Evans, R.H. and H. Gordon, Coastal zone color scanner system calibration: A retrospective examination, *J. Geophys. Res., 99*, 7293-7307, 1994.

Herman, J.R., P.K. Bhartia, O. Torres. C. Hsu, C. Seftor, and E. Celarier, Global distributions of UV-absorbing aerosols from Nimbus 7/TOMS data, *J. Geophys. Res., 102*, 16911 -16923, 1997.

Higurashi, A. and T. Nakajima, Development of a Two Channel Aerosol Retrieval Algorithm on Global Scale Using NOAA / AVHRR, *J. Atmos. Sci., in press*, 1998.

Holben, B.N., A. Setzer, T.F. Eck, A. Pereira, and I. Slutsker, Effect of dry-season biomass burning on Amazon basin acrosol concentrations and optical properities, *J. Geophys. Res., 101*, 19465-19481, 1996.

Husar, R.B., J.M. Prospero, and L.L. Stowe, Characterization of tropospheric aerosols over the oceans with the NOAA advanced very high resolution radiometer optical thickness operational product, *J. Geophys. Res., 102*, 16889-16910, 1997.

IPCC95, *Climate Change 1995: The Science of Climate Change*, J.T. Houghton, L.G.M. Filho, B.A. Callander, N. Harris, A. Katternberg, and K. Maskell (eds.), 572pp., Cambridge Univ. Press., New York, 1996.

Kaufman, Y.J. and B.N. Holben, 1996: Hemispherical backscattering by biomass burning and sulfate particles derived from sky measurements, *J. Geophys. Res., 101*, 19433-19445.

Kaufman, Y.J., A. Gitelson, A. Karnieli, E. Ganor, R.S. Fraser, T. Nakajima, S. Mattoo, and B.N. Holben, Size distribution and scattering phase function of aerosol particles retrieved from sky brightness measurements, *J. Geophys. Res., 99*, 10341-10356, 1994.

Langner, J., H. Rodhe, P.J. Crutzen, and P. Zimmermann, Anthropogenic influence on the distribution of tropospheric sulphate aerosol, *Nature, 359*, 712-717, 1992.

Moulin, C., C.E. Lambert, F. Dulac, and U. Dayan, Control of atmospheric export of dust from North Africa by the North Atlantic Oscillation, *Nature, 387*, 691-694, 1997.

Nakajima, T., and A. Higurashi, AVHRR remote sensing of aerosol optical properties in the Persian Gulf region, the summer 1991, *J. Geophys. Res., 102*, 16935-16946, 1997.

Nakajima, T., G. Tonna, R. Rao, Y. Kaufman, and B. Holben, Use of sky brightness measurements from ground for remote sensing of particulate polydispersions, *App. Opt., 35*, 2672-2686, 1996.

Nakajima, T., M. Tanaka, M. Yamano, M. Shiobara, K. Arao and Y. Nakanishi, Aerosol optical characteristics in the yellow sand events observed in May, 1982 in Nagasaki - Part II Model, *J. Meteor. Soc. Japan, 67*, 279-291, 1989.

Patterson, E.M. and D.A. Gillette, Commonalities in measured size distributions for aerosols having a soil-derived component, *J. Geophys. Res., 82*, 2074-2082, 1977.

Penner, J.E. and T. Novakov, Carbonaceous particles in the atmosphere: A historical perspective to the Fifth International Conference on carbonaceous particles in the atmosphere, *J. Geophys. Res., 101*, 19373-19378, 1996.

Pollack, J.B., and J.N. Cuzzi, Scattering by nonspherical particles of size comparable to a wavelength: A new semi-empirical theory and its application to tropospheric aerosols, *J. Atmos. Sci., 37*, 868-881, 1980.

Shiobara, M., T. Hayasaka, T. Nakajima and M. Tanaka, Aerosol monitoring by use of a scanning spectral radiometer in Sendai, Japan, *J. Meteor. Soc. Japan, 69*, 57-70, 1991.

Sokolik, I., A. Andronova, and T.C. Johnson, 1993: Complex refractive index of atmospheric dust aerosols. *Atmos. Environ., 16*, 2495-2502.

Tanré, D., C. Devaux, M. Herman and R. Santer, Radiative properties of desert aerosols by optical ground-based measurements at solar wavelengths, *J. Geophys. Res., 93*, 14223-14231, 1988.

Twomey, S., The influence of pollution on the shortwave albedo of clouds, *J. Atmos. Sci., 34*, 1149-1152, 1977.

A. Higurashi, National Institute for Environmental Studies, 16-2 Onogawa, Tsukuba, Ibaraki 305-0053, Japan. (e-mail: hakiko@nies.go.jp)

T. Nakajima, Center for Climate System Research, University of Tokyo, 4-6-1 Komaba, Meguro-ku, Tokyo 153-8904, Japan. (e-mail: teruyuki@ccsr.u-tokyo.ac.jp)

(Received December 15, 1997; Revised April 21, 1998; accepted June 8, 1998.)